Geochemical Characteristics and Significance of Major Elements, Trace Elements and REE in Mineralized Altered Rocks of Large-Scale Tsagaan Suvarga Cu-Mo Porphyry Deposit in Mongolia

Fang Weixuan (方维萱)[1,2]*, Yang Shefeng (杨社锋)[2], Liu Zhengtao (刘正桃)[1], Wei Xinglin (韦星林)[3], Zhang Baochen (张宝琛)[1]

(1. Beijing Technological Center of Resource Exploration, China Non-Ferrous Metals Geological Survey, Beijing 100012, China; 2. State Key Laboratory of Deposit Geochemistry, Chinese Academy of Sciences, Guiyang 550002, China; 3. Jiangxi Provincial Non-Ferrous Metals Geological Survey, Nanchang 330001, China)

Abstract: The alteration types of the large-scale Tsagaan Suvarga Cu-Mo porphyry deposit mostly comprise stockwork silicification, argillization, quartz-sericite alteration, K-silicate alteration, and propylitization. The mineralized and altered zones from hydrothermal metallogenic center to the outside successively are Cu-bearing stockwork silicification zone, Cu-bearing argillized zone, Cu-Mo-bearing quartz-sericite alteration zone, Cu-Mo-bearing K-silicate alteration zone, and propylitization zone. The K-silicate alteration occurred in the early phase, quartz-sericite alteration in the medium phase, and argillization and carbonatization (calcite) in the later phase. Ore-bearing-altered rocks are significantly controlled by the structure and fissure zones of different scales, and NE- and NW-trending fissure zones could probably be the migration pathways of the porphyry hydrothermal system. Results in this study indicated that the less the concentrations of REE, LREE, and HREE and the more the extensive fractionation between LREE and HREE, the closer it is to the center circulatory hydrothermal ore-forming and the more extensive silicification. The exponential relationship between the fractionation of LREE and HREE and the intensity of silicification and K-silicate alteration was found in the Cu-Mo deposit studied. The negative Eu anomaly, normal Eu, positive Eu anomaly and obviously positive Eu anomaly are coincident with the enhancement of Na_2O and K_2O concentrations gradually, which indicated that Eu anomaly would be significantly controlled by the alkaline metasomatism of the circulatory hydrothermal ore-forming system. Therefore, such characteristics as the positive Eu anomaly, the obvious fractionation between LREE and HREE and their related special alteration lithofacies are suggested to be metallogenic prognostic and exploration indications for Tsagaan Suvarga-style porphyry Cu-Mo deposits in Mongolia and China.

Key words: mongolia; tsagaan suvarga porphyry Cu-Mo deposit; wall rock alteration; fractionation mode; positive Eu anomaly; rare earths

CLC number: P618.51; P595   **Document code:** A   **Article ID:** 1002 – 0721(2007)06 – 0759 – 11

Rare earth elements (REE) and their related geochemical parameters are used for metallogenic and liquid-geochemical tracing because all the REE display very similar geochemical behaviors[1~12]. However, REE and their geochemical parameters for alteration lithofacies in the porphyry environment, especially

exploration indications of their parameters and related alteration lithofacies on porphyry system have been poorly understood up to now. Furthermore, there is little report available on comparisons between Tsagaan Suvarga porphyry Cu-Mo deposit in South Gobi in Mongolia and porphyry Cu-Mo deposits in the East Tianshan in China, although porphyry Cu-Mo-Au deposits have been found in the East Tianshan in China, recently[13~24]. Therefore, a better understanding of the potential of prospecting porphyry Cu-Mo-Au deposits from the East Tianshan to the Beishan in China is necessary. On the basis of the geochemistry of REE and trace elements in altered rocks in Tsagaan Suvarga porphyry Cu-Mo deposit, the characteristics of the alteration of wall rocks and fractionations of REE as well as trace elements were discussed, and the comprehensive exploration indicators of REE were summarized.

1 General Geology

Located in the central Asian orogenic belt of the Late Paleozoic active continental margin of Tianshan of China to South Gobi of Mongolia, and in mature magmatic island arc zone of Andean-type continental island arc, Tsagaan Suvarga porphyry Cu-Mo deposit is one of the most typical porphyry Cu-Mo deposit within the Au-Cu-Mo-Fe metallogenic system in this continental margin (Fig. 1). Tsagaan Suvarga porphyry Cu-Mo deposit has the same geotectonic setting as Tuwu-Yandong porphyry deposits in China. In the area studied, Devonian lithological associations consists of marine andesite, dacite, dacitic rhyolite, sili-

ceous rock of abyssal facies, jasper rock and proclastic sedimentary rock with partially interbedded carbonate rock, which are characterized by typical lithological associations of active continental margin island arc. In the carboniferous marine facies, the terrigenous sedimentary system and volcanic rocks of littoral facies are composed of andesite-dacite, dacite-rhyolite and carbonate rock, tuff, terrigenous clastic rock, basic, intermediate and acid subalkaline rocks of continental facies and clastic rock series developed well. Furthermore, rock assemblages of typical mature island arc lithological association include basalt, basaltic andesite, andesite, dacite, rhyolite, basaltic trachyte, trachyte, trachytic basalt, trachyandesite, andesite-rhyolite-trachytic rhyolite, sandstone and siltstone. These rock series and the lithological association indicate that continental collision happened and oceanic basin was closed in this area in the Carboniferous period. Distributions of the Late Carboniferous and the Early Permian marine andesite-dacite, dacite-rhyolite and terrigenous clastic rocks interbedded by carbonate rock show that the residual paleo-ocean basin was being shrunk, whereas the Late Carboniferous and the Early Permian lithological associations of basaltic trachyte, trachyte, trachytic basalt, trachyandesite and esite-rhyolite-trachytic rhyolite indicate that the residual volcanic island arc and subduction and collision remained in the area studied. However, rock assemblages of ore-bearing intrusive complex intrusions which covers an area of 90 km^2 contain gabbro, diorite, syenodiorite, granodiorite and leucogranite and syenititic porphyry . This complex intrusion, plunges into the
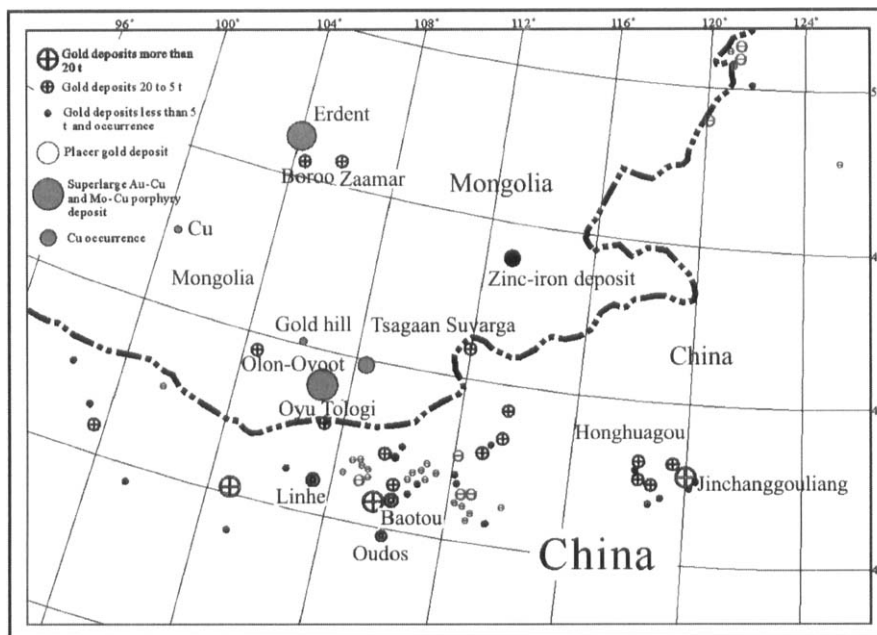

Fig. 1. Schematic location map of Tsagaan Suvarga Cu-Mo porphyry deposit in south Mongolia

NW direction and extends underneath the carboniferous volcanic-sedimentary rock series, whereas structural contact zone was reported between the complex intrusions and their wall rocks. Factually, structural contact zones were host bodies of cryptoexplosive breccia, whereas Cu-Mo orebodies were hosted in the northern part of cryptoexplosive breccia bodies.

Tsagaan Suvarga porphyry Cu-Mo deposit ranks the third largest porphyry Cu deposits in Mongolia, with Cu and Mo metal resource being a tonnage of 1.5 million and 0.05 million at average grades of 0.72% Cu and 0.023% Mo, respectively. It is also accompanied with Se and Au, with Se metal resource of 1992 tonnes at an average grade of 8.3 g · t^{-1} Se. The observed mineralized zone is 2000 m long, 450 m wide and 250 m deep. Copper and Mo mineralized zone is hosted within argillic, silicification and quartz-sericite alteration zones between the carboniferous two monzonitic porphyry veins, and the Cu-Mo ore are mainly in veinlet and disseminating texture hosted in dense fissure zones. In fact, there is much sericite alteration on the walls of sulfide-quartz veinlets. Moreover, fine sulfide veinlets and disseminated chalcopyrite-molybdenite-silicification-sericite alteration occur as fissure fillings in small extensive altered ribbons which are found along the high-intensity fissures of granodiorite. In addition, molybdenite mostly occurs inside and outside the walls of chalcocite-chalcopyrite-quartz veinlets, and along the walls of fissures in K-silicate altered rocks. Ore minerals in oxidized zone consist mainly of malachite, limonite, bornite, chalcocite, covellite and azurite, whereas ore minerals in primary zone are mainly chalcopyrite, molybdenite, pyrite, magnetite, hematite, galena and sphalerite, of which pyrite is intergrowth with galena, sphalerite and tennantite. Ore minerals in primary zone are enriched in quartz-sericite and silicification alteration zones. Gangue minerals mostly comprise quartz, sericite, potash feldspar, kaolinite, dickite, chlorite and calcite.

The metallogenic date of Tsagaan Suvarga porphyry Cu-Mo deposit is considered to be in the Late Devonian age. According to a report by Lamb and Cox (1998)[16], ^{40}Ar/^{39}Ar age of muscovite from K-silicate alteration zone in ore-bearing porphyry is 364.9 ± 3.5 Ma, and the weighed average ^{40}Ar/^{39}Ar age of non-altered monzonitic porphyry is (313.0 ± 5.8) Ma. The monzonitic porphyry intersected the Cu-Mo mineralized zone, indicating that mineralization occurred 313.0 ± 5.8 Ma ago. Re-Os age of molybdenite from K-feldspar altered granite is (370 ± 0.8) Ma. It is close to the age of muscovite. Because

the accuracy of dating from molybdenite is better than that of muscovite, the mineralized date of this deposit is considered to be in the Late Devonian period.

2   Sample and Analytical Method

Sampling sites were measured by portable GPS. Samples were processed in the workshop of the Institute of Geochemistry, Chinese Academy of Sciences. Major elements were analyzed with pure chemical quantitative method, whereas trace elements and REE were analyzed in Analysis Laboratory, Beijing Institute of Uranium Geology through HR-ICP-MS (Element I) made by Finning MAT.

3   Geochemical Characteristics of Major Elements, Trace Elements and REE of Cu-Mo-Bearing Altered Rocks

3.1   Geology and geochemistry of major elements, trace elements and REE of Cu-Mo-bearing altered rocks

Ore-forming intrusive bodies are mainly composed of Cu-Mo-bearing altered granodiorite, dioritic porphyry, altered gabbro-diorite and porphyritic gabbro. (1) Alteration types are mainly silicification, argillization of stockwork, quartz-sericite alteration, K-silicate alteration and propylitic alteration. (2) The mineralized and altered zoning from the hydrothermal metallogenic center to the outside part observed on the surface is Cu-bearing stockwork silicification zone, Cu-bearing argillized zone, Cu-Mo bearing quartz-sericite alteration zone, Cu-Mo bearing K-silicate alteration zone and propylitization zone respectively, whereas the mineralized and altered zoning from the depth to the surface is, Cu-Mo-bearing K-silicate alteration zone, Cu-Mo-bearing quartz-sericite alteration zone, Cu-Mo-bearing stockwork silicification zone and Cu-bearing argillized zone, respectively. (3) The K-silicate alteration occurs in the early stage, quartz-sericite and silicified alteration in the medium stage, and argillization and carbonatization (calcite, siderite) in the later stage. Ore-bearing altered rocks are obviously dominated by structure and fissure zones of different scales. Veinlet and stockwork silicified alterations are controlled by small-scale fractures, whereas other mineralized and alterations are directed by high-density fissures in which sulfides are filled well. These sulfides mainly exist as quartz-sulfides and quartz-sericite-sulfide veinlets. Distribution of the stockwork ore bodies is controlled by NE- and NW-trending fissure zones with veinlet ore zone of 10 ~ 20 m in depth and several hundred meters in

length. These possibly indicate that NE- and NW-trending fissure zones would probably migrate through pathways for hydrothermal ore-forming system in the porphyry environment. Thus, it can be supposed that the most intense mineralized and alteration might occur in intersections of NE- and NW-trending fissure zones, which are indicated by the deep part of the weakly NE-trending structural zone intersected by the NW-trending fracture. Their different geochemical characteristics of major and trace elements from ore-bearing altered rocks are summarized as follows:

1. Propylitic altered rock: The assemblages of altered minerals consist of assemblages of epidote + chlorite ± carbonate, which is well developed in diorite and the carboniferous volcanic rocks (wall rocks). The carboniferous rocks do not display an obvious Cu-Mo mineralization only with banded and planar pyrite on the periphery of the ore-bearing altered zones in the area studied.

2. K-silicate altered rock (TS1, TS5, TS4, TS8): The assemblage of altered minerals is the assemblage of potash feldspar + chlorite + sericite ± quartz ± biotite. The original intermediate feldspars are mainly K-feldspars and secondly sericitization, whereas K-silicate alteration is exhibited in the porphyritic gabbro, gabbro-diorite, diorite, dioritic porphyry and granodiorite-porphyry. (1) Melanic minerals such as pyroxene and hornblende account for about 80% of the total minerals in the total volume in Cu-bearing altered porphyritic gabbro, whereas most of the grayish basic feldspar is altered into the reddish potash feldspar (accounting for 15% of total volume). (2) The dark-colored minerals (30%) in Cu-bearing altered dioritic porphyry and gabbro-diorite had already been altered into the chlorites which still remains a crystalline pseudomorph of hornblende, pyroxene and biotite. The pseudomorph of some dark-colored minerals remains phenocryst with 2 ~ 5 cm in length and 0.5 ~ 2 cm in breadth. Phenocryst of medium-basic feldspar had been altered into potash feldspar most of which is red and some of which remains grayish. (3) K-silicate alteration in the Cu-bearing granodioritic porphyry and dioritic porphyry is in the form of veinlet and stockwork along fissure zones. (4) A great amount of chalcopyrite, bornite, molybdenite and some sphalerite were formed. Fine veinlet-disseminated sulfide is presented along the fine fissures in K-silicate rocks with the width of the veinlet ranging from 5 to 10 mm, and their density from 100 to 150 pieces of ore-bearing fissures per meter.

Fine veinlet-disseminated sulfides filled in the

fissures of greenish-gray Cu-bearing diorite with weak alteration (TS5) and grading of 0.83% Cu, 2422 × 10^{-6} Zn, 16.7 × 10^{-6} Cd and 6.99 × 10^{-6} Mo indicates that copper is enriched in the greenish-gray altered diorite (TS5) in an environment of the fracturation and hydrothermal alteration for diorite.

In comparison with the greenish-gray diorite of weak alteration (TS5), the characteristics of the major elements of K-silicate zone (Table 1) are characterized by higher concentrations of K_2O (5.52% ~ 5.61%) and SiO_2 (64.61% ~ 67.93%), lower concentrations of Na_2O (2.39% ~ 4.64%), as well as CaO, MgO, Fe_2O_3 and FeO. Furthermore, the ranges of K_2O/Na_2O ratios, concentrations of ($K_2O + Na_2O$) and SiO_2/K_2O ratios are 1.89 ~ 2.35, 8.00% ~ 10.21% and 11.9 ~ 12.3, respectively. Copper mineralization yields at the grades of 0.36% ~ 0.87%. The anomalous values of ore-forming elements such as Mo ((6.05 ~ 211) × 10^{-6}), Zn (2422 × 10^{-6}) and Bi (11.4 × 10^{-6}) are locally found. These data are evidences of the fact that K-silicate alteration may produce Cu enrichment or Cu mineralization accumulation, in which most of the Cu-bearing ores with lower grades are coincident with local Mo, Zn and Bi enrichments. Fig. 2 illustrates that large ion lithophile element (LILE) in K-silicate rocks (TS4, TS8) are typified by remarkable positive U-K, La and Pb anomaly, negative Th, Ta-Nb, Sr and Sm anomaly, and depletion of high-field strength cations such as Ta-Nb.

The characteristics of the Cu-bearing gabbro with weak alteration (TS1, Figs. 2 and 3) comprises K-silicate alteration, slight silicification and magnetite alteration, and they were superimposed by argillization and white carbonation (calcite) of the late stage along microfissure of gabbro. Obviously, fracturation, enrichment of LILE, visible positive anomaly of U-K and La-Ce-Pb and Sm, evident negative anomaly of Sr and Ti and P, as well as relative depletion of high-field strength cations such as Ta-Nb are found inside, and the altered gabbro has the same characteristics of high V (572 × 10^{-6}) as primary gabbro.

3. Silicification-sericite altered rocks (TS6, TS7 and TS16): Altered mineral assemblage is composed of quartz + sericite ± potash feldspar ± chlorite. (1) Silicification-sericite alteration is distributed around K-silicate altered rocks consisting of Cu-Mo-bearing potash feldspar-quartz-sericite altered rocks and quartz-sericite altered rocks, making it difficult to identify their protolith. (2) Stockwork and veinlet (0.5 ~ 2.5 cm in width) of potash feldspar is common in locally transitional parts of K-silicate altered rock and silicification-sericite altered rocks, and they main-

ly comprise Cu-Mo-bearing potash feldspar-quartz-sericite altered rocks. Moreover, they mainly comprise quartz and sericite with gradual disappearance of the potash feldspar while enhancing the quartz and sericite alteration. (3) Strong silicification-sericite altered rocks in grayish-white color distribute along the fractures and fissures. When stronger silicification occurs locally in the form of stockwork silicification (1 ~ 1.5 cm wide) and is superimposed on banded silicified-sericite altered zone, it is obvious for sulfide to concentrate highly. (4) In quartz-sericite altered rocks, sulfide (chalcopyrite, bornite, molybdenite and minor sphalerite) is distributed in the form of fine veinlet dissemination (0.2 ~ 0.3 cm in width) and is partially disseminated along the fine fissures with 133 ~ 160 pieces of fissures per meter.

As for the characteristics of major elements (Table 1), K_2O concentrations range from 3.28% to 5.61% and Na_2O from 0.99% to 2.39%, the concentrations of which is obviously lower. However, concentrations of $K_2O + Na_2O$ are not high, ranging from 4.27% to 8.00%, mainly caused by complete potash metasomatism. Ratios of SiO_2/K_2O are high because potash feldspar is altered by sericite owing to the enhancement of silicification-sericite alteration. Some values of metallogenic elements such as Cu (2.08% ~ 4.43%), Mo ((399 ~ 1591) $\times 10^{-6}$), Zn (3579 $\times 10^{-6}$), Cd (11.4 $\times 10^{-6}$), W((20.2 ~ 25.2) $\times 10^{-6}$) and local U (56.3 $\times 10^{-6}$) show that Cu-Mo are largely enriched and ores of higher Cu grade or high Cu-Mo grade are yielded associating with an enrichment of Zn, Cd, W and U.

As shown in Fig. 2, LILE are still enriched in the silicification-sericite altered rocks (TS6, TS7, TS16), but high-field strength cations such as Ta-Nb is relatively depleted with obvious positive U, La-Ce-Pb anomaly. Negative Sr anomaly exhibits with the enhancement of silicification-sericite alterations.

4. Vein-stockwork silicification altered rock: Altered mineral assemblage consists of quartz + sericite.
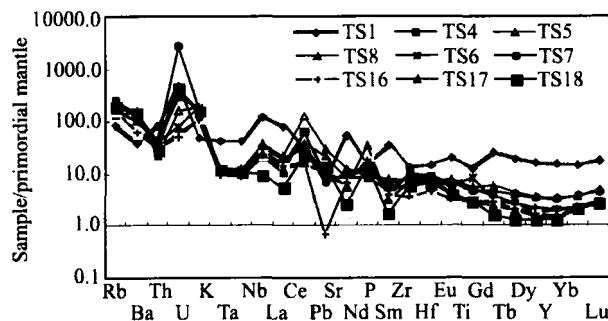

Fig. 2 Spider diagram of large iron lithophile elements in mineralized and altered rocks in Tsagaan Suvarga Cu-Mo porphyry deposit

The metallogenic centre consists of vein and veinlet chalcopyrite-bornite-silicified veins, openly controlled by fractures, within fractures of silicified-sericite altered rock. This metallogenic centre is the best-hosted dimension of copper ores at higher Cu grades, which can be exemplified by identification symbols of convective circulatory metallogenic centre for the porphyry system. The main characteristics are summarized as follows:

(1) Chalcopyrite quartz veins (TS11, TS13) are 2 ~ 5 cm in width. The small massive and disseminated chalcopyrite and other sulfide are formed in the same stage as that in the silicification. Fine fissures of 2 ~ 5 mm in width, averaging 130 pieces per meter, are well developed in quartz veins, filled by fine veinlet-disseminated chalcopyrite and bornite. Therefore, the latter may be formed later than the former. Concentrations of SiO_2 range from 76.5% to 79.28%, Al_2O_3 from 6.04% to 7.07% and K_2O from 0.23% to 1.47% in chalcopyrite quartz veins. The higher concentrations of Al_2O_3 and K_2O are principally related to the sericite developed in the quartz veins and on their vein walls. Concentrations of copper are up to 3.07 to 4.98% in these quartz veins, with a maximum of 43645 $\times 10^{-6}$ Zn, 73.8 $\times 10^{-6}$ Bi, 563 $\times 10^{-6}$ Mo and 2.08% TiO_2, as well as Se from 5.63 $\times 10^{-6}$ to 27.3 $\times 10^{-6}$. Chalcopyrite-molybdenite quartz veins are distributed in local with Mo maximum up to 6046 $\times 10^{-6}$. All of these indicate that the strong silicification zone is the ore-forming center in the area studied.

(2) Molybdenite occurs in the form of membrane, irregular small massive, dissemination, and fine veinlet-dissemination in fine fissures (2 ~ 5 mm in width) of quartz veins (TS12) of 2 ~ 5 cm in width. The fine fissures of 2 ~ 5 mm in width and at the density of 160 pieces of fine fissures per meter are well developed in the quartz veins which contain Cu grading of 0.7%, Mo grading of 8417 $\times 10^{-6}$, TiO_2 grading of 1.0% and CaO grading of 4.55%. CaO is mainly derived from carbonate minerals and the features are coincident with calcite, and results from the late
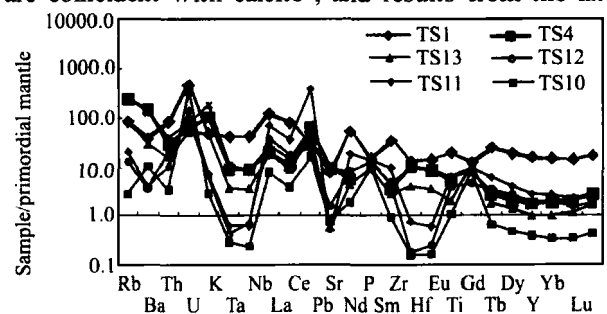

Fig. 3 Spider diagram of LILE in altered rocks in Tsagaan Suvarga Cu-Mo porphyry deposit

superimposed alteration.

(3) Malachite and chalcocite quartz veins, general 5 ~30 cm in width with the maximal width up to 73 cm, are common at the surface in the area studied. Stockwork, disseminated and small massive malachite and malachite-chalcocite occur in quartz veins which are well developed in argillic zone and argillic hematite-ochre alteration zone at the surface.

Up to 5.67% Cu, 43645 ×10^{-6} Zn, 27.3 ×10^{-6} Se, 73.8 ×10^{-6} Bi, 1508 ×10^{-6} Mo and 1.75% TiO$_2$ are found in these veins. However, the LILE are enriched in these veins (TS10, TS11, TS12, TS13), with obvious positive anomaly of U, La-Ce-Pb, Nd-P-Sm, Eu-Ti and apparent depletion of Ta-Nb, Sr, Zr-Hf (Fig. 3).

Table 1 Major elements (%, mass fraction) and trace elements (×10^{-6}) composition of mineralized and altered rocks in Tsagaan Suvarga Cu-Mo porphyry deposit in south Mongolia

Sample	TS1	TS5	TS4	TS8	TS6	TS7	TS16	TS13	TS12	TS11	TS10	TS17	TS18
SiO$_2$	56.46	59.98	67.93	64.61	66.99	68.72	69.23	79.28	88.82	76.5	87.16	61.97	66.67
TiO$_2$	2.75	1.75	1.17	1.13	1.76	1.04	0.64	2.5	1.0	2.08	1.75	0/61	0.64
Al$_2$O$_3$	9.85	18.19	16.67	17.68	16.42	15.66	13.88	7.07	0.25	6.04	1.25	15.91	15.91
Fe$_2$O$_3$	7.57	1.8	0.4	0.15	0.67	0.6	3.35	2.01	0.2	3.6	0.2	0.42	1.0
FeO	4.1	0.7	0.1	0.05	0.1	0.27	1.06	0.79	0.05	0.94	0.05	0.1	0.37
MnO	0.24	0.07	0.6	0.07	0.22	0.03	0.04	0.08	0.1	0.19	0.05	0.02	0.06
MgO	2.83	1.31	0.01	0.25	0.15	0.21	0.42	0.01	0.01	0.21	0.01	0.35	0.18
CaO	5.63	2.78	0.77	1.9	0.67	1.74	0.44	0.96	4.55	0.66	0.59	0.43	0.35
Na$_2$O	1.32	5.14	2.92	4.64	2.39	1.03	0.99	0.08	0.01	0.21	0.01	2.29	5.21
K$_2$O	1.42	3.23	5.52	5.57	5.61	5.42	3.28	1.47	0.21	0.23	0.09	4.22	4.92
P$_2$O$_5$	0.33	0.37	0.2	0.19	0.28	0.27	0.4	0.21	0.28	0.3	0.21	0.77	0.3
Ignition loss	6.24	3.21	2.85	2.79	2.26	2.6	1.3	1.91	3.24	3.54	3.71	7.27	3.04
Cu	0.87	0.83	0.36	0.39	2.18	2.08	4.43	3.07	0.7	4.98	5.67	5.55	1.0
Total	99.61	96.15	99.5	99.42	99.7	99.67	99.46	99.44	99.41	99.27	99.75	99.91	99.65
V	572	102	158	54.8	86.3	109	85.3	108	20.6	8.38	32.8	103	55.7
Cr	10.7	4.23	9.87	10.4	3.7	8.15	7.58	12.3	17.8	11.6	14.4	8.93	11.1
Co	18.6	1.51	7.14	2.23	2.28	1.89	4.63	2.43	2.08	7.48	3.87	1.03	0.985
Ni	8.79	1.42	4.4	2.97	1.39	2.07	1.59	1.93	5.29	1.86	1.92	1.24	1.77
Zn	152	2422	72.2	36.3	3579	46.7	24.9	34.8	509	43645	108	28.9	30.8
Ga	28.1	21.7	23.1	17.8	20.1	19.8	18.7	8.48	3.19	5.54	1.22	18.2	14.3
Ge	4.61	0.725	1.21	0.702	0.63	0.86	0.76	0.629	0.664	1.61	0.283	0.442	0.388
As	1.4	0.438	0.606	0.459	0.263	0.35	0.425	0.224	0.315	2.55	1.19	0.242	0.42
Se	13.7	3.85	4.45	1.39	3.92	3.97	6.45	5.65	3.82	27.3	5.53	5.16	2.66
Rb	53.7	153	84.5	123	160	161	105	56.1	8.29	13	1.8	107	120
Sr	166	203	633	469	190	147	14.1	11.7	33.7	11.2	16.9	221	294
Y	68.4	8.79	15.7	9.14	9.24	14.8	7.07	4.62	8.94	12.4	1.57	5.85	6.06
Zr	148	114	83.7	69.8	111	93.4	40.8	45.3	2.03	8.58	1.82	75.5	63.9
Nb	30.4	6.48	7.94	6.84	6.09	6.85	6.5	2.57	0.502	0.466	0.174	8.59	7.81
Mo	64	16.7	6.05	211	27.3	1591	399	6046	8147	563	1508	19.8	558
Cd	0.414	6.99	0.131	0.9	11.4	5.92	2.15	27.3	41.3	198	6.97	0.215	2.33
In	0.146	0.059	0.109	0.032	0.061	0.13	0.283	0.356	0.381	18.1	0.174	0.054	0.121
Sn	1.75	0.668	1.09	0.988	2.03	4.7	5.45	3.2	0.523	0.581	3.16	2.69	0.424
Sb	0.198	0.407	0.083	0.105	0.358	0.094	0.055	0.182	0.193	5.55	0.308	0.061	0.204
Ba	268	1044	1073	1030	880	938	416	204	26.4	28.5	73.4	709	1021
Hf	4.49	2.7	2.19	1.94	2.78	2.51	1.42	1.1	0.079	0.191	0.051	2.65	2.05
Ta	1.71	0.378	0.379	0.388	0.438	0.383	0.392	0.151	0.018	0.026	0.012	0.515	0.495
W	3.95	6.6	5.54	6.11	10.9	25.2	20.2	6.03	1.7	1.65	1.23	9.3	6.05
Pb	5.68	11.9	23.1	6.94	11.5	5.83	3	7.87	4.62	70.2	3.08	2.94	4.2
Bi	1.45	0.297	11.4	0.118	0.625	1.14	1.1	0.305	1.18	73.8	0.574	3.43	0.274
Th	7.13	2.61	1.87	3.44	3.38	3.74	2.63	1.32	1.85	0.886	0.308	3.66	2.46
U	9.66	1.3	3.4	6.14	1.65	56.3	1.06	1.13	1.81	2.87	7.5	9.37	8.94

Table 2 Rare earth element ($\times 10^{-6}$) and their ratios of mineralized and altered rocks in Tsagaan Suvarga Cu-Mo porphyry deposit in south Mongolia

Sample	TS-1	TS4	TS5	TS8	TS6	TS7	TS16	TS13	TS12	TS11	TS10	TS17	TS18
La	85.2	13.5	25.2	18	18.7	22.2	15.6	12.8	25.9	47.7	5.35	15.5	6.48
Ce	142	19.4	39.2	28	27.3	34.3	24.6	15.8	31.5	64.5	7.0	22.3	9.7
Pr	17.9	2.22	4.62	2.99	3.07	3.71	2.69	1.69	3.3	6.63	0.767	2.22	0.949
Nd	70.7	8.04	17.3	11.2	11.3	14.1	9.34	6.19	11.3	25.3	2.65	7.77	3.57
Sm	15.1	1.59	3.53	2.11	2.12	2.71	1.76	1.23	2.15	4.42	0.438	1.39	0.759
Eu	3.35	0.902	1.29	1.1	1.03	1.12	0.542	0.349	0.684	1.08	0.19	0.656	0.658
Gd	14.9	1.69	3.61	2.2	1.91	2.87	1.68	1.11	2.08	3.72	0.407	1.48	0.986
Tb	2.08	0.221	0.458	0.296	0.275	0.429	0.222	0.152	0.285	0.451	0.052	0.209	0.14
Dy	11.8	1.33	2.65	1.61	1.46	2.46	1.23	0.76	1.46	2.1	0.292	1.07	0.937
Ho	2.43	0.294	0.558	0.339	0.315	0.537	0.268	0.179	0.301	0.417	0.057	0.23	0.223
Er	7.26	0.919	1.71	0.983	0.979	1.69	0.851	0.538	0.865	1.26	0.163	0.713	0.783
Tm	1.24	0.168	0.317	0.178	0.186	0.304	0.16	0.1	0.154	0.206	0.032	0.147	0.161
Yb	7.18	1.0	1.87	1.09	1.06	1.88	1.01	0.616	0.785	1.17	0.176	0.991	1.08
Lu	1.28	0.206	0.359	0.199	0.218	0.339	0.193	0.123	0.137	0.186	0.032	0.197	0.202
REE	382	51.5	103	70.3	69.9	88.6	60.1	41.6	80.9	159	17.6	54.9	26.6
LREE	334	45.7	91.1	63.4	63.5	78.1	54.5	38.1	74.8	150	16.4	49.8	22.1
HREE	48.2	5.83	11.5	6.90	6.40	10.5	5.61	3.58	6.07	9.51	1.21	5.04	4.51
LR/HR	6.94	7.83	7.90	9.20	9.92	7.44	9.71	10.6	12.3	15.7	13.5	9.89	4.90
$(La/Yb)_N$	8.00	9.1	9.1	11.1	11.9	8.0	10.4	14.0	22.2	27.5	20.5	10.5	4.0
δ_{Eu}	0.68	1.67	1.10	1.55	1.54	1.22	0.95	0.90	0.98	0.79	1.35	1.39	2.33
K_2O/Na_2O	1.08	0.63	1.89	1.2	2.35	5.26	3.31	18.4	21	1.1	9.0	1.84	0.94
$K_2O + Na_2O$	2.74	8.37	8.44	10.21	8.0	6.45	4.27	1.55	0.22	0.44	0.1	6.51	10.1
SiO_2/K_2O	39.8	18.6	12.3	11.6	11.9	12.7	21.1	53.9	423	333	968	14.7	13.6
Fe^{2+}/Fe^{3+}	0.60	0.43	0.28	0.37	0.17	0.50	0.35	0.44	0.28	0.29	0.28	0.26	0.41

5. Argillized altered rocks: The altered mineral assemblage comprises kaolinite, dickite, hydromica, hematite and ochre which are distributed around the area of vein-veinlet chalcopyrite-bornite-silicification center consisting of hematite-ochre argillization altered rock and malachite argillization altered rock.

The argillized rocks contain Cu from 1% to 5%, Na₂O from 2.29% to 5.21%, and K₂O from 4.22 to 4.92%. Whereas, LILE are enriched in argillized altered rocks (TS17, TS18) with obvious positive anomaly of U-K, Pb, P and Zr-Hf and obvious negative anomaly of Ta-Nb-La-Ce, Nd and Sm (Fig. 2).

To summarize, the relationship between Cu-Mo ore-forming and wall-rock alteration can be further better understood as follows. (1) Copper is mainly enriched in the quartz-sericite altered rock, argillized altered rock and silicified rock resulting in copper ores at higher grades, while copper is mineralized in the potash silicate altered rock at lower grades. Moreover, Mo enrichment has the same law as Cu. It shows that Cu-Mo ore-forming has a close relationship with the quartz-sericite altered rock, argillized altered rock and silicified rock. Hence the geochemical anomaly of Cu-Mo-Zn covering the quartz-sericite, argillized, silicified and the potash-silicate altered rocks is an exploration mark for this type of Tsagaan Suvarga porphyry Cu-Mo deposit. On the other hand, mature island arc zone and associations of indicator elements including

Cu, Mo, Zn, In, Cd, Bi and W are geological and geochemical prospecting indicators. (2) Concentrations of SiO₂ increases from 59.98% to 87.16%, and Al₂O₃ decreases from 18.19% to 0.25% and Na₂O from 5.14% to minimum of 0.01% from grayish-green diorite with slight alteration (TS5) to potash-silicate alteration rock, to quartz-sericite altered rock and to vein-veinlet silicified altered rock, indicating that SiO₂ was continuously brought in and accumulated, and Ba, Al₂O₃ and Na₂O were continuously taken out and migrated with an increase of SiO₂/K₂O ratios continuously from peripheral margins of convective metallogenic hydrothermal circulatory fluids to the metallogenic center in the porphyry environment. Therefore, the vein and veinlet silicified rocks and anomaly of Cu, Mo, Zn, In, Cd, Bi and Se associations are indicators of the metallogenic center in the porphyry environment. (3) The loss on ignition (LOI) of argillized rock of malachite alteration (TS17) is the highest at 7.27% among all the rocks, but concentrations of CaO and MgO are very low, implying the presence of a few carbonate minerals. These results are identical and are proved by the slice observation under microscope; therefore LOI is mainly attributed to hydroscopic water. It suggests that much hydroscopic water in argillized alteration zone could be closely related with atmospheric precipitation in the shallow part underground.

3.2 Geochemical characteristics of REE

(1) Totally (Table 3), all samples in this study are featured by LREE enrichment with REE ranging from 41.6×10^{-6} to 382×10^{-6}, LREE from 38.1×10^{-6} to 334×10^{-6} and HREE from 1.21×10^{-6} to 48.2×10^{-6}. (2) Obvious fractionation is between LREE and HREE with ratios of LR/HR ranging from 4.9 to 15.7, and $(La/Yb)_N$ value from 4.0 to 27.5. (3) Ore-bearing altered gabbro has a remarkable negative Eu anomaly with $\delta_{Eu} = -0.68$. Ore-bearing K-silicate, silicified-K silicate and argillized altered rocks have a remarkable positive Eu anomaly with δ_{Eu} from 1.1 to 2.22. Ore-bearing vein-veinlet silicified altered rocks have a slight negative Eu anomaly with δ_{Eu} ranging from 0.79 to 0.98.

The different geochemical characteristics of REE from various ore-bearing altered rocks are as follows:

1. Concentrations of REE in ore-bearing gabbro of slight alteration (slight silicified-K silicate altered zone with broken fissures, TS1, Table 3, Fig. 4) has the highest value with concentrations of REE up to 382×10^{-6}, and has LREE enriched at 334×10^{-6} with concentrations of HREE being 48.2×10^{-6}. The ore-bearing altered gabbro has a remarkable negative Eu anomaly with δ_{Eu} at -0.68. Obvious fractionation

between LREE and HREE is presented by ratios of LR/HR = 6.94 and $(La/Yb)_N = 8.0$.

2. The concentration of REE of slightly K-silicate-altered rock (TS4) is 103×10^{-6} with an inconspicuous positive Eu anomaly ($\delta_{Eu} = 1.10$). However, concentrations of REE range from 51.5×10^{-6} to 70.3×10^{-6}, whereas K silicification (TS5, TS8) and positive Eu anomaly ranging from 1.55 to 1.67 are enhanced.

3. Concentrations of REE are less than 100×10^{-6} in the silicification-sericite altered rock (TS6, TS7) with an enrichment of LREE and a positive Eu anomaly. Eu is inconspicuously depleted (TS16) whereas silicification is further promoted.

4. Eu is depleted significantly in vein and veinlet silicified rocks (TS10, TS11, TS12 and TS13) although ratios of LR/HR ranging from 10.6 to 15.7 and ratios of $(La/Yb)_N$ ranging from 14.0 to 27.5 are obviously increased. It displays that the fractionation between LREE and HREE is the most conspicuous.

5. Ratios of LR/HR = 4.9 and $(La/Yb)_N = 4.0$, respectively, in argillized rock (TS18) illustrate that the fractionation between LREE and HREE is the slightest. However, distributions of REE has W-pattern in the REE abundant plot with $\delta_{Eu} = 2.33$.
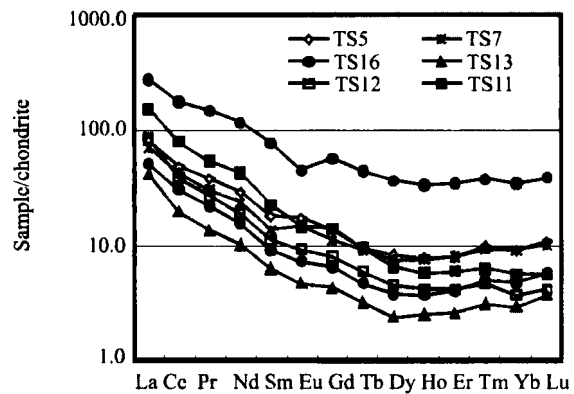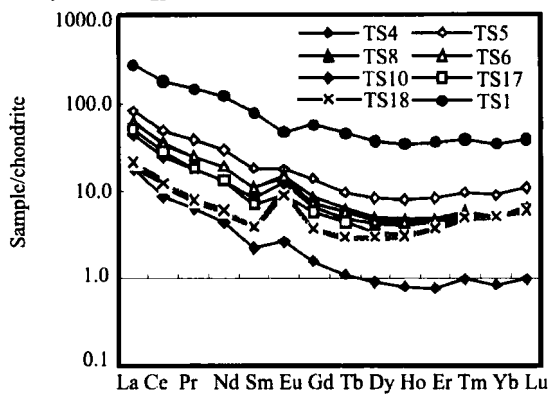

Fig. 4   REE abundances in Tsagaan Suvarga porphyry deposit, normalized to Chondrite values
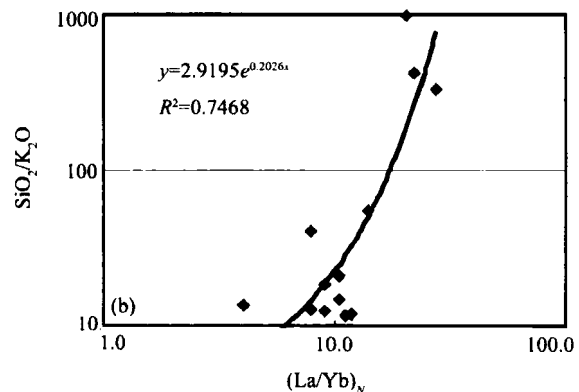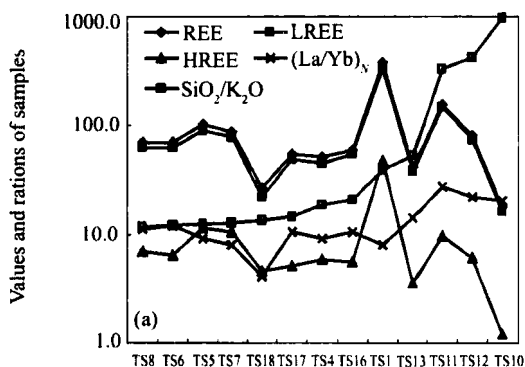

Fig. 5   A plot of values vs. sample number (a) and a log-log bivariate plot of SiO_2/K_2O ratios vs. $(La/Yb)_N$ (b) from the data presented in Table 2

4 Discussion

1. As a whole, concentrations of REE are decreased and the fractionation between LREE and HREE becomes obvious (Fig. 5, Table 3) with continuous silicification enhancement. The convective circulatory center of ore-forming fluids in the porphyry system could be indicated by the chalcopyrite-bornite- silicification veins and veinlet and it is also the center of the fractionation between LREE and HREE. These data possibly show that the geochemical and geological characteristics of the center place significance in prospecting prognosis. The extent of the fractionation between LREE and HREE can be reflected by the concentrations of REE, LREE, HREE and ratios of $(La/Yb)_N$. The ratios of SiO_2/K_2O possibly indicate a different degree of silicification in comparison with K-silicate alteration in ore-bearing altered rocks. Concentrations of REE, LREE, HREE and ratios of $(La/Yb)_N$ have an obviously decreasing trend, whereas ratios of SiO_2/K_2O an increasing trend (Fig. 5). It shows that the concentrations of REE, LREE and HREE decrease, and the fractionation extent between LREE and HREE is enhanced when silicification is continually intensified. There is an exponential relation between the fractionation extent of LREE and HREE and the silicification-K silicate alteration, and the exponential relation can be mathematically simulated by the following formula:

$y \ (SiO_2/K_2O) = 2.9195 e^{0.2026x}$, $x = (La/Yb)_N$,

Total number of samples = 14

R (simulated correlation coefficient) = 0.862.

2. One typical characteristic of the ore-bearing K silicate, silicified K silicate and argillized altered rocks is a remarkable positive Eu anomaly. There is no obvious law of relation of the values of SiO_2/K_2O and the positive Eu anomaly (Table 3). In view of the above-mentioned high SiO_2/K_2O and strong silicification being, the fractionation center of LREE and

HREE, the relation between the Eu anomaly and other alteration types can be studied. Hence, the positive Eu-anomaly-forming mechanism can be discussed accordingly without regard to vein-veinlet silicified altered rocks. The Eu anomaly has a significant positive correlation with $Na_2O + K_2O$ of the ore-bearing altered rocks, which represents an extent of the alkaline metasomatism of altered rocks (Fig. 6). Because the Eu anomaly changes from negative anomaly to normal, further to positive anomaly and distinctly positive anomaly while $Na_2O + K_2O$ continually increases, it shows that the Eu anomaly is obviously controlled by alkaline metasomatism of circulatory hydrothermal metallogenic system. Ration of Fe^{2+}/Fe^{3+} is generally a correlative trend with the positive Eu anomaly; as shown, the positive Eu anomaly is related with alkaline-oxidizing metallogenic environment. However, the relation of the Eu anomaly and K_2O/Na_2O, local change of Fe^{2+}/Fe^{3+} calls for further research.

3. It is well known that the magma-hydrothermal system of the high emplacement of porphyry Cu deposits[25~30] is featured by a high oxygen fugacity with tracing minerals indicating a higher oxygen fugacity such as magnetite, hematite, gypsum and anhydrite as well as daughter minerals such as hematite and chalcopyrite in mineral fluid inclusion[31]. Ratios of Fe^{2+}/Fe^{3+} in the area studied ranges from 0.17 to 0.6 (Table 3) with developed magnetite and hematite, suggesting that metallogenic fluids have a higher oxygen fugacity. Magnetite-altered rock (lithofacies) is also an important alteration type of wall rock and one of the ore-prospecting signs[32~34], which offers a material prerequisite for prospecting for the porphyry Cu deposit by means of magnetic method. Magnetite alteration developed in a highly oxidized magma-hydrothermal system is associated with K-silicate altered rock of the early phase; possibly for Fe-bearing dark-colored minerals after potash feldspar and sericite alteration causes much precipitation and accumulation of
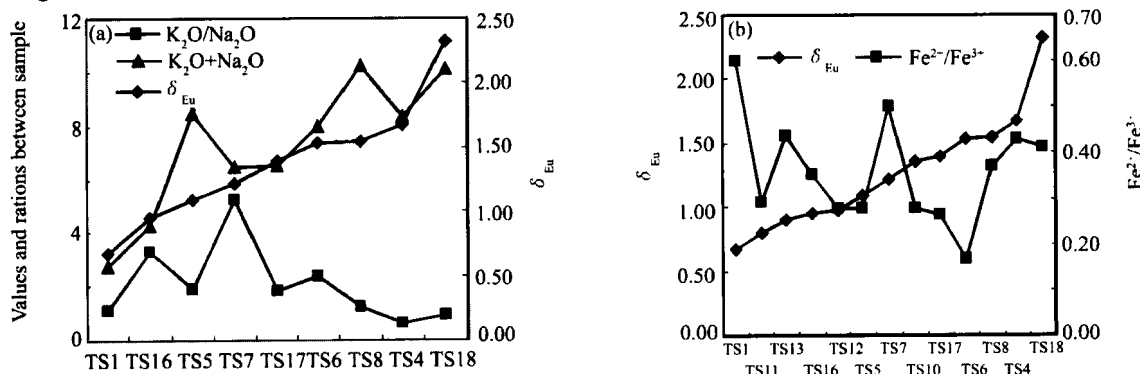

Fig. 6 Plots of values vs. sample number showing relationship of $Na_2O + K_2O$ and Eu anomaly, data from Table 2
(a) Relationship of $(Na_2O + K_2O)$ and Eu anomaly; (b) Relationship of (Fe^{2+}/Fe^{3+}) and Eu anomaly

Fe^{2+} and Fe^{3+} to form magnetite alteration. This area studied has the concordant characteristics with known high emplacement of magma-hydrothermal system of porphyry Cu deposits.

4. The zoning characteristics of mineralized and altered zones from hydrothermal metallogenic center to periphery in this area are Cu-bearing stockwork silicification zone, Cu-bearing argillized zone, Cu-Mo-bearing quartz-sericite alteration zone, Cu-Mo-bearing K-silicate alteration zone and propylitization zone, and have similar alteration characteristics and zoning to the general porphyry Cu deposits[35,36]. A peculiar characteristic is mineralized altered gabbro and superimposition of late argillic and carbonate alteration to the gabbro. This is different from Tangling area and Sauer region in China[37,38].

5 Conclusions

In summary, the relationship between Cu-Mo ore-forming and wall-rock alteration in the area studied was as follows:

1. Cu-Mo ore-forming could be closely related to the quartz-sericite alteration, argillization and silicification. LILE were enriched in mineralized altered rocks with an obviously positive anomaly of U-K, La and Pb, a negative anomaly of Ta-Nb and a relative depletion of high-field strength elements (HFSE) such as Ta-Nb.

2. Vein-veinlet silicified rocks and composite anomaly of Cu-Mo-Zn-In-Cd-Bi-Se in geochemical prospecting are the prognostication markers of metallogenic center of porphyry-circulatory hydrothermal system of this type. Decreased REE and the distinct fractionation between LREE and HREE showed that the convective circulatory center of ore-forming fluids in porphyritic metallogenic system which was composed of veinlet chalcopyrite-bornite-silicification altered and mineralized veins, was the center of the fractionation between LREE and HREE.

3. The contents of REE, LREE and HREE decreased, and the fractionation extent between LREE and HREE was enhanced when silicification was continually intensified. There was an exponential relation between the fractionation extent of LREE and HREE and the silicification-K silicate alteration.

4. The Eu anomaly changed from negative anomaly to normal, further to positive anomaly and distinctly positive anomaly, whereas $Na_2O + K_2O$ continually increase. It showed that the Eu anomaly was obviously controlled by the alkaline metasomatism of the circulatory hydrothermal metallogenic system. Such characteristics as a positive Eu anomaly, distinct

fractionation between LREE and HREE and relevant wall-rock alteration features, were prognostic indices for the similar prospect areas to Tsagaan Suvarga large-scale porphyry Cu-Mo deposit in Mongolia.

References:

[1] Whitney Philip R, Olmsted James F. Rare earth element metasomatism in hydrothermal systems: The Willsboro-Lewis wollastonite ores, New York, USA [J]. *Geochimica et Cosmochimica Acta*, 1998, 62(17): 2965.

[2] Yang Xueming, Yang Xiaoyong, Chen Tianhu, Zhang Peishan, Tao Kejie. Geochemical characteristics of a carbonatite dyke rich in rare earths from Bayan Obo, China [J]. *Journal of the Chinese Rare Earth Society* (in Chin.), 1999, 17(4): 289.

[3] Pang Jiangli, Sun Gengnian. Geochemical behaviour of rare earth elements in Jianchaling deposit, Shaanxi Province [J]. *Journal of the Chinese Rare Earth Society* (in Chin.), 1999, 17(4):359.

[4] Pang Jiangli. Geochemistry of rare earth elements in hydrothermal ore deposit in Heishan area, Shaanxi province[J]. *Journal of Rare Earths*, 1999, 19(1): 53.

[5] Huang Zhilong, Xiao Huayun, Xu Cheng, Liu Congqiang. Geochemistry of rare earth elements in lamprophyres in Laowangzhai gold orefield, Yunnan province[J]. *Journal of Rare Earths*, 2000, 18(1): 62.

[6] Chen Tianhu, Yang Xueming, Yue Shucang, Li Shuangying, Wang Daoxuan. Geochemistry of rare elements in Xikeng Ag Pb Zn ore deposit, South Anhui, China[J]. *Journal of Rare Earths*, 2000, 18(3):169.

[7] Yuan Feng, Zhou Taofa, Liu Xiaodong, Yue Shucang. Geochemistry of rare earth elements of Anqing copper deposit in Anhui province[J]. *Journal of Rare Earths*, 2002, 20(3): 223.

[8] Zhang Zhanshi, Hua Renmin, Liu Xiaodong, Deng Ping, Wu Lieqin. Geochemical characteristics of rare earth elements of guidong granitic complex and their relationship with uranium mineralization [J]. *Journal of the Chinese Rare Earth Society* (in Chin.), 2005, 23(3): 749.

[9] Yang Fenggen, Wang Henian, Hua Renmin. Transportation of REE in ductile shear zone in Hetai gold deposit [J]. *Journal of the Chinese Rare Earth Society* (in Chin.), 2004, 22(1): 164.

[10] Xie Qiaoqin, Xu Xiaochun, Li Xiaoxuan, Chen Tianhu. Rare earth elements geochemistry of Laowan gold deposit in Henan Province : Trace to source of ore-forming materials[J]. *Journal of Rare Earths*, 2006, 24(1): 115.

[11] Zhang Hong, Zhang Qi. Rare earths, trace element characteristics of high-Mg volcanic rocks of Yixian Formation in Sihetun West Liaoning Province and its apocalypse[J]. *Journal of Rare Earths*, 2005, 23(4): 502.

[12] Ling Qicong, Liu Congqiang. Review of rare earths and fluid-rock interaction [J]. *Journal of Rare Earths*, 2002, 20(6): 570.

[13] Perello J, Cox D, Garamjav D, Sanjdorj S, Diakov S, Schissel Munkhbat, Oyun T G. Oyu Tolgoi, Mongolia: Siluro-Devonian porphyry Cu -Au-(Mo) and high-

sulfidation Cu mineralization with a Cretaceous chalco-
cite blanket [J]. *Economic Geology*, 2001, **96**: 1407.

[14] Gombosuren B, Cunningham D W, Windley B F.   A
new terrane subdivision for Mongolia: implications for
the Phanerozoic crustal growth of Central Asia [J].
Journal of Asian Earth Sciences, **21**: 87.

[15] Badarch, Cunningham G, Windley W D, Tomurtogoo B
F.   Tectonics and geodynamic evolution of Mongolia
[J]. *Mongolia Geoscientist*, 2003, **21**: 1.

[16] Lamb M A, Cox D.   New ^{40}Ar/^{39}Ar age data and im-
plications for porphyry copper deposits of Mongolia
[J]. *Economic Geology*, 1998, **98**: 524.

[17] Watanabe Y, Stein J.   Re-Os ages for the Erdenet and
Tsagaan Suvarga porphyry Cu-Mo deposits, Mongolia,
and tectonic implications [J]. *Economic Geology*, 2000,
95: 1537.

[18] Lowell J D, Guilbert J M.   Lateral and vertical altera-
tion-mineralization zoning in porphyry ore deposits
[J]. *Economic Geology*, 1970, **65**: 373.

[19] Zhang Lianchang, Qin Kezhang, Ying Jifeng, Xia Bin,
Shu Jiansheng.   The relationship between ore-forming
processes and adakitic rock in Tuwu-Yandong porphyry
copper metallogenic belt, eastern Tianshan mountains
[J]. *Acta Petrologica Sinica* (in Chin.), 2004, **20** (2):
259.

[20] Yang Xingke, Cheng Hongbing, Ji Jinsheng, Chen Qiang,
Luo Gulchang.   Analysis on gold and copper ore-form-
ing system with collision orogeny of eastern Tianshan
[J]. *Geotectonica Et Metallogenia* (in Chin.), 1999, **23**
(4): 315.

[21] Xiao W J, Zhang L C, Qin K Z, Sun S, Li J L.   Paleo-
zoic accretionary and collision tectonics of the eastern
Tianshan (China): Implications for the continental
growth of central Asia [J]. *American Journal of Sci-
ence*, 2004, **304**: 370.

[22] Rui Zongyao, Wang Futong, Li Henghai, Dong Lianhui,
Wang Lei, Jiang Lifeng, Liu Yulin, Wang Longsheng,
Chen Weishi.   The new advances of research on Dong-
tianshan belt of porphyry Cu deposits [J]. *Chinese
Geology* (in Chin.), 2001, **28**(2): 11.

[23] Wang Futong, Feng Jing, Hu Jianwei, Wang Lei, Jiang
Lifeng, Zhang Zheng.   The characteristics and signifi-
cance of Tuwu large scale porphyry Cu deposit in Xin-
jiang Uigur Autonomous Region [J]. *Chinese Geology*
(in Chin.), 2001, **28**(1): 36.

[24] Zhang Lianchang, Wan Bo, Li Wenqian, Tang Hongfeng.
Geochemistry and tectonic setting of copper-bearing
porphyries on the southern margin of Tuha basin, Xin-
jiang [J]. *Acta Petrologica Sinica* (in Chin.), 2006, **22**
(1): 225.

[25] Sillitoe R H.   Characteristics and controls of the largest
porphyry copper-gold and epithermal gold deposits in
the circum-Pacific region [J]. *Australian Journal of
Earth Sciences*, 1997, **44**: 373.

[26] Tarkian M, Stribrny B.   Platinum-group elements in
porphyry copper deposit , a reconnaissance study [J].
Mineralogy and Petrology, 1999, **65**: 161.

[27] Gammons C H, Bloom M S , Yu Y.   Experimental in-
vestigation of the hydrothermal geochemistry of plati-
num and palladium: I Solubility of platinum and palla-
dium sulphide minerals in NaCl/H$_2$SO$_4$ solutions at 300
℃ [J]. *Geochimica et Cosmochimica Acta*, 1992, **56**: 3
881.

[28] Rui Zongyao, Zhang Lisheng, Chen Zhenyu, Wang
Longsheng, Liu Yulin, Wang Yitian.   Approach on
source rock or source region of porphyry copper depos-
its [J]. *Acta Petrologica Sinica* (in Chin.), 2004, **20**(2):
229.

[29] Streck J M , Dilles J H.   Sulfur evolution of oxidized
arc magmas as recorded in apatite from a porphyry cop-
per batholith[J]. *Geology*,1998, **26**: 523.

[30] MacDonald G D, Arnold L C.   Geo logical and geo-
chemical zoning of the Grasberg igneous complex, Irian
Jaya, Indonesia [J]. *J. of Geochemical Exploration*,
1994, **50**: 143.

[31] Lu Huanzhang.   High temperature, salinity and high
concentrated ore metal magmatic fluids: an example from
Grasberg Cu-Au porphyry deposit [J]. *Acta Petrologi-
ca Sinica* (in Chin.), 2000, **16**(4): 465.

[32] Arancibia O N , Clark A H.   Early magnetite-amphi-
bole-plagioclase alteration-mineralization in the Island
Copper porphyry copper-gold-molybdenum deposit,
British Columbia [J]. *Economic Geology*,1996, **91**:
402.

[33] Fountain R J.   Geological relationships in the Panguna
porphyry copper deposit, Bougainville Island, New
Guinea [J]. *Economic Geology*, 1972, **67**: 1049.

[34] Mealey G A.   Grasberg: Mining the richest and most
remote deposit of copper and gold in the world, in the
mountains of Irian Jaya, Indonesia[M]. New Orleans:
Produced and published by Freeport-McMoRan Cop-
per & Gold Inc., 1996. 1.

[35] Lowell J D, Guilbert J M.   Lateral and vertical altera-
tion-mineralization zoning in porphyry ore deposits[J].
Econmic, Geology, 1970, **65**: 373.

[36] Hollister V F, Potter R R, Barker A L.   Porphyry-
type deposits of appalachian orogen [J]. *Economic Ge-
ology*, 1974, **69**: 618.

[37] Xu Xiaochun, Lu Sanming, Xie Qiaoqin, et al.   Rare
earth element geochemistry on magmatic rocks and gold
deposits in Shizishan ore field of Tongling, China [J].
Journal of Rare Earths, 2006, **24**(5): 617.

[38] Tan Lugui, Zhou Taofa, Yuan Feng, Fan Yu, Yue Shu-
cang.   Mechanism of formation of Premian volcanic
rocks in Sawu′er region, Xinjiang, China: constraints
from rare earth elements [J]. *Journal of Rare Earths*,
2006, **24**(5): 626.